De Novo Production of the Bioactive Phenylpropanoid Artepillin C Using Membrane-Bound Prenyltransferase in Komagataella phaffii

Bamba, Takahiro ; Munakata, Ryosuke ; Ushiro, Yuya ; Kumokita, Ryota ; Tanaka, Sayaka ; Hori, Yoshimi ; Kondo, Akihiko ; Yazaki, Kazufumi ;…

(Citation)
ACS Synthetic Biology,13(12):4040-4049

(Issue Date)
2024-11-12

(Resource Type)
journal article

(Version)
Accepted Manuscript

Title:

***De novo* production of the bioactive phenylpropanoid artepillin C using membrane-bound prenyltransferase in *Komagataella phaffii*.**

Authors:

Takahiro Bamba[1,†], Ryosuke Munakata[2,†], Yuya Ushiro[3], Ryota Kumokita[3], Sayaka Tanaka[3], Yoshimi Hori[1], Akihiko Kondo[1,3,4], Kazufumi Yazaki[2,*], Tomohisa Hasunuma[1,3,4,*]

Author Affiliations:

[1] Engineering Biology Research Center, Kobe University, 1-1 Rokkodai, Nada, Kobe, 657-8501, Japan

[2] Laboratory of Plant Gene Expression, Research Institute for Sustainable Humanosphere, Kyoto University, Uji 611–0011, Japan

[3] Graduate School of Science, Technology and Innovation, Kobe University, 1-1 Rokkodai, Nada, Kobe 657-8501, Japan

[4] RIKEN Center for Sustainable Resource Science, 1-7-22 Suehiro-cho, Tsurumi-ku, Yokohama, Kanagawa 230-0045, Japan

† These authors equally contributed to this research

* Corresponding authors

Corresponding authors:

Kazufumi Yazaki

Laboratory of Plant Gene Expression, Research Institute for Sustainable Humanosphere, Kyoto University, Uji 611–0011, Japan

Telephone: +81-774-38-4504; Fax: +81-774-38-3623

E-mail: yazaki@rish.kyoto-u.ac.jp

Tomohisa Hasunuma

Graduate School of Science, Technology and Innovation, Kobe University

1-1 Rokkodai, Nada, Kobe 657-8501, Japan

Telephone: +81-78-803-6461; Fax: +81-78-803-6461

E-mail: hasunuma@port.kobe-u.ac.jp

Abstract

Artepillin C is a di-prenylated phenylpropanoid with various pharmacological benefits for human health. Its natural occurrence is limited to a few Asteraceae plants like *Baccharis* species, necessitating a stable supply through synthetic biology. In *Saccharomyces cerevisiae*, the utilization of aromatic substrates within the cell was limited, resulting in very low production of artepillin C. In this study, we used AcPT1, a *p*-coumaric acid (*p*-CA)-specific di-prenyltransferase, in *Komagataella phaffii* to produce artepillin C. Detailed studies revealed that the critical bottleneck in *K. phaffii* was the supply of prenyl diphosphates, not phenylpropanoid flux. By enhancing the prenyl substrate pathway through overexpression of isopentenyl diphosphate isomerase and a truncated HMG-CoA reductase, we achieved a strong increase in artepillin C production. A major part of artepillin C was accumulated in yeast cells. One of the advantages of *K. phaffii* is its superior growth and ability to achieve high cell density cultivation compared to *S. cerevisiae*. Therefore, fed-batch cultivation with glycerol was performed. As a result, the dry cell weight (DCW) reached 61.0 g/L and the intracellular amount of *de novo* produced artepillin C reached 187.3 μg/DCW. Analysis of intermediates revealed that the supply of *p*-CA constituted a bottleneck in artepillin C production in the engineered strain. By enhancing *p*-CA supply, the intracellular accumulation of artepillin C reached 1200 μg/DCW even in batch cultivation. Moreover, the total intra- and extracellular amount of artepillin C reached 12.5 mg/L, marking the highest *de novo* synthesis amount of artepillin C reported thus far, even under batch cultivation conditions.

Keywords

Komagataella phaffii, metabolic engineering, prenyltransferase, prenylated phenolic

compounds, artepillin C, high cell density cultivation

Introduction

More than 4,000 prenylated phenolic compounds occur in plant secondary metabolism[1]. Many of them have been identified as biologically active compounds in a variety of medicinal plants, and they have also been reported to play a role in plant chemical defense against herbivores and pathogens. As the former example, 8-prenylated naringenin in Fabaceae shows prevention of disuse atrophy[2], auraptene (a geranylated coumarin) in *Citrus* species inhibits Epstein Barr virus[3], and hyperforin (a polyprenylated acylphloroglucinol) in *Hypericum* spp. shows antidepressant activity[4]. The latter example represents a co-evolutionary arms race between plants and herbivores mediated by a series of prenylated coumarin derivatives called linear and angular furanocoumarins[5]. It should be emphasized that these activities are increased, sometimes dramatically, by the addition of prenyl residue(s) compared to the non-prenylated parent compounds[3]. Despite these attractive properties as compounds, these prenylated compounds exist as complex mixtures of similar derivatives and/or the content of each substance is often very low in plants. These are the reasons, at least in part, why most prenylated phenolic compounds are not used as dietary supplements or mild medicines to support human health.

Based on the above, valuable prenylated phenolic compounds have become attractive targets in synthetic biology. Indeed, the production of some prenylated phenolics by synthetic biology has been reported[6–8]. For example, the anticancer and anticarcinogenic flavonoid icariin from *Epimedium* species and the psychoactive compounds tetrahydrocannabinols from *Cannabis sativa* have been constructed[6,7]. However, the production level of those compounds was not sufficient for industrial production. In synthetic biology for the production of prenylated phenolics, one of the major hurdles is that the key enzymes of prenylation are membrane-bound proteins with typically nine transmembrane alpha helices[9], belonging to the UbiA superfamily. Thus, reasonable expression at the protein level is difficult even when using the yeast host. Another difficulty is the identification of aromatic prenyltransferase (PT) genes specific for the target prenylated phenolics. Plant aromatic PTs, especially in secondary metabolism, generally have strict specificity in both substrate recognition and prenylation position for core phenolic compounds.

In this study, we chose artepillin C, a di-prenylated p-coumaric acid (*p*-CA), as the target compound, which is a plant secondary metabolite known to be the major active compound in Brazilian green propolis, a globally available apicultural product[10,11]. The pharmacological activities of artepillin C have been intensively studied, i.e. antimicrobial[10], anti-inflammatory[12], antioxidant[11], modulation of immune responses[13], anticancer activities[14,15]. Another important finding is that this compound shows an activity to convert white adipocytes into brown-like adipocytes when administered to mice via a master regulator of adipocyte differentiation, peroxisome proliferator-activated receptor gamma, suggesting that artepillin C has beneficial effects on obesity and diabetes in humans[16].

The chemotaxonomy of this compound is rather narrow and limited to some species of the Asteraceae. *Baccharis dracunculifolia*, the botanical origin of artepillin C in Brazilian green propolis, is mainly distributed in South America[17,18]. Due to this limitation, we have previously identified the UbiA-type PT gene AcPT1 responsible for the production of artepillin C from a medicinal plant *Artemisia capillaris* native to Japan. This enzyme has the unique property that this single protein can successively transfer two prenyl residues from dimethylallyl diphosphate (DMAPP) to *p*-CA as its specific substrate to form artepillin C[19]. In our previous report, we attempted to produce artepillin C in *Saccharomyces cerevisiae*, however the production level was only approximately 4 μmol/L (1.2 mg/L). Even when an excess of the prenyl acceptor substrate *p*-CA was added to the medium, the artepillin C production reached approximately 68 μmol/L (20 mg/L). We also observed that approx. 90% of the artepillin C produced was retained in the yeast cell fraction. In synthetic biology approach, selection of host organism is another key to produce the compound of interest. Here, we have selected another host, *Komagataella phaffii* (*Pichia pastoris*), for the production of this di-prenylated phenylpropanoid using AcPT1.

K. phaffii has several attractive properties compared to *S. cerevisiae* in bioproduction. *K. phaffii* is a Crabtree-negative yeast that does not produce ethanol even under aerobic conditions and has superior growth ability compared to *S. cerevisiae*[20–22]. Our previous study reported that *K. phaffii* has a superior ability to produce aromatic compounds such as flavonoids and benzylisoquinoline alkaloids[23]. In addition, *K. phaffii* can be cultured at high cell densities[24,25]. Therefore, it must be possible to significantly increase the production amount per cultivation scale for intracellularly accumulated compounds such as artepillin C. In this study, we first demonstrated that artepillin C can be produced in *K. phaffii* by introducing tyrosine ammonia-lyase (TAL) and AcPT1 without any addition of *p*-CA. We then investigated the effect on artepillin C production of increasing the supply of the precursor *p*-CA and the prenyl group

donor DMAPP. This study also demonstrated that high cell density cultivation of *K. phaffii* in a jar fermentor is useful for artepillin C production. Finally, based on the results of high cell density cultivation, we worked on further improving the artepillin C-producing strain.

Results

Introduction of artepillin C biosynthetic pathway into *K. phaffii*

The biosynthetic pathway of artepillin C is shown in Figure 1. For artepillin C production, two major pathways should be coupled, i.e., the shikimate pathway to provide *p*-CA, the prenyl acceptor substrate, via tyrosine, and DMAPP via the mevalonate pathway[23]. The coupling step is catalyzed by the membrane-bound PT AcPT1. In budding yeast, however, it has been reported that *p*-CA was mostly excreted into the medium (approximately 10 mg/L), with only 1% (0.1 mg/L) remaining in the cells[19]. Thus, this low intracellular level of *p*-CA in *S. cerevisiae* is disadvantageous for use as a substrate for the prenylation reaction in vivo. In this study, we used the *Herpetosiphon aurantiacus*-derived TAL, which increases the efficiency of providing *p*-CA in vivo. The *HaTAL* was integrated into the *K. phaffii* strain CBS7435Δ*dnl4*Δ*his4*. The resulting *K. phaffii* strain successfully produced *p*-CA. After 96 h of cultivation, the amount of *p*-CA in the medium was 69 ± 1 mg/L (mean ± SD), while the amount of *p*-CA accumulated in the cells was 11.0 ± 0.4 mg/L per unit volume of medium (mean ± SD). The retention rate of *p*-CA in the cells was observed to be 15% (Fig. 2A), which is more favorable for the production of artepillin C than in *S. cerevisiae*, which retains only about 1% of the produced *p*-CA in the cell fraction[19].

Artepillin C is produced from *p*-CA by di-prenylation of AcPT1. Since AcPT1 is localized in plastids in plant cells, this protein has a transit peptide (TP) at the N-terminus for plastid sorting, but in general yeast cells do not have a strong tolerance to TP and these N-terminal extensions cause protein instability or misfolding. In fact, it has been reported that the removal of TPs from plant aromatic PTs leads to an increase in the activity of recombinant proteins in the *S. cerevisiae* expression system, *e.g.*, *Lupinus alba* PT1 (6-fold)[26] and *Citrus limon* PT-1 (6-fold)[27]. When AcPT1 was expressed in *S. cerevisiae*, removal of its TP resulted in a detectable yield of artepillin C[19]. Therefore, we compared the productivity of artepillin C between the full-length AcPT1 and a TP-truncated AcPT1 (tTP_AcPT1) in the TAL-introduced *K. phaffii* strain. In our previous study, we examined the components of the medium and carbon sources, and the results suggested that the YP + glycerol (YPG) medium is advantageous for the production of *p*-CA

derivatives in *K. phaffii*[28]. Therefore, in this study, we used the YPG medium for the production of artepillin C. As a result, artepillin C was accumulated in yeast cells from 48 h and increased with cultivation time (Fig. 2A). The accumulation amount of artepillin C was 3.9 ± 0.2 and 4.3 ± 0.3 μg/g-DCW (means ± SDs) at 144 h in TAL-AcPT1 and TAL-tTP_AcPT1 strains, respectively. However, the effect of removing the TP sequence was not significant in *K. phaffii*. The reason may be that the plant TP sequence does not interfere with protein folding in *K. phaffii*, or the actual effect was not observed due to the depletion of substrate supply in vivo. It should be noted that when we analyzed the culture media, artepillin C was not detected in the medium. This is probably due to the high hydrophobicity of this compound.

Enhancement of shikimate pathway on artepillin C production

As a next step, we investigated the rate-limiting reactions for the production of artepillin C. In the tyrosine upstream pathway, the *S. cerevisiae* 3-deoxy-D-arabino-heptulosonate-7-phosphate synthase ARO4 and the chorismate mutase ARO7 are subject to negative feedback from tyrosine[29–31]. We then created a mutant ARO4 in which Lys229 was replaced with Leu ($ARO4^{K299L}$), and a mutant ARO7 in which Gly141 was changed to Ser ($ARO7^{G141S}$), both of which are insensitive to negative feedback from tyrosine. These mutant genes were then driven by the glyceraldehyde-3-phosphate dehydrogenase (GAP) promoter to enhance the metabolic flux from tyrosine to *p*-CA in the TAL-AcPT1 strain. The amounts of intra- and extracellular *p*-CA and the amount of artepillin C were compared between TAL-AcPT1 and TAL-AcPT1-ARO47m (Fig. 3AB). As expected, the amounts of intracellular and extracellular *p*-CA were apparently increased by the introduction of $ARO4^{K299L}$ and $ARO7^{G141S}$, whereas the accumulation of intracellular artepillin C was slightly decreased. In addition, no artepillin C was detected in the culture medium for either strain. The glycerol consumption profile was almost the same for both strains, on the other hand, cell growth was slightly worse in the TAL-AcPT1-ARO47m strain (Fig. 3C). These results suggest that the supply of *p*-CA is not a rate-limiting factor for artepillin C production. The reason why the expression of $ARO4^{K299L}$ and $ARO7^{G141S}$ was ineffective for artepillin C production is unclear, but one possibility is that this forced metabolic change increased the aromatic amino acids while suppressing the other amino acids such as alanine and glycine in *S. cerevisiae*. This disturbance in the amino acid balance may cause a slight disadvantage in the cell growth and artepillin C production.

Enhancement of DMAPP supply to increase artepillin C production

We then tried to increase the DMAPP supply in vivo. A rate-limiting reaction step in the mevalonate pathway is catalyzed by hydroxymethylglutaryl (HMG)-CoA reductase (HMG1)[32]. This enzyme is localized to the endoplasmic reticulum through its N-terminal transmembrane domain, which is involved in the protein degradation as a regulatory mechanism of this important reaction step[33]. Since the removal of this domain (339 amino acids) suppresses the degradation of HMG1, we prepared the truncated HMG1 (tHMG1) and overexpressed it to increase the DMAPP pool. Moreover, as DMAPP forms an equilibrium state with its isomer IPP by isopentenyl diphosphate delta-isomerase (IDI1). It has been reported that the overexpression of *IDI1* increases the DMAPP/IPP ratio[34]. We then introduced these genes into the TAL-AcPT1 strain to establish the strains TAL-AcPT1-tHMG1, TAL-AcPT1-IDI1, and TAL-AcPT1-tHMG1-IDI1 strains. Figure 4 shows the time courses of artepillin C production in these strains. Artepillin C production was observed 48 h after initiation of the culture, and artepillin C production was increased in all these strains, in which the DMAPP pool is enhanced (Fig. 4). In particular, the overexpression of *IDI1* showed a strong effect, and in the TAL-AcPT1-tHMG1-IDI1 strain overexpressing both *tHMG1* and *IDI1*, a 24-fold increase in artepillin C production was achieved compared to the TAL-AcPT1 strain after 120 h of culture (3.3 ± 0.4 and 80 ± 10 μg/g-DCW (mean ± SD), respectively) (Fig. 4A). It is also noteworthy that artepillin C release into the culture medium was observed in the TAL-AcPT1-tHMG1-IDI1 strain. Artepillin C was detected at 72 h, and the level increased during cultivation (Fig. 4B). The amount of artepillin C reached 0.14 ± 0.02 mg/L (mean ± SD) after 144 h. This suggests that the cells cannot retain artepillin C in the cellular fraction due to its high production. Taken together, the prenyl substrate supply is suggested to be a critical rate-limiting pathway in *K. phaffii*, and the enhancement of the DMAPP pool largely contributed to the artepillin C production.

Artepillin C production through fed-batch cultivation using a jar fermentor

A significant accumulation of artepillin C in the cells was observed even in the strain with increased DMAPP supply. One of the characteristics of *K. phaffii* is its ability to be cultured at high densities. However, a preliminary experiment showed that the CBS7435*Δdnl4Δhis4* strain, which was used as the parental strain in this study, achieved a significantly lower OD in fed-batch cultivation with glycerol using a jar fermentor compared to the CBS7435 WT strain (Fig. S1). The *DNL4* encoded the DNA ligase IV homolog and its disruption improves the efficiency

of homologous recombination in *K. phaffii*[35]. The *HIS4* is a gene involved in histidine synthesis, and its disruption has the advantage of allowing the use of *HIS4* as an auxotrophic marker gene. However, the disruption of these two genes is not necessarily required for the construction of artepillin C producing strains. Therefore, the artepillin C producing strain (W-TAL-AcPT1-tHMG1-IDI1 strain) was reconstructed using CBS7435 WT as the parental strain. The result of flask batch cultivation, the W-TAL-AcPT1-tHMG1-IDI1 strain showed a higher OD throughout the cultivation compared to the TAL-AcPT1-tHMG1-IDI1 strain (Fig. S2). The intracellular and extracellular production of artepillin C was almost the same for both strains up to 96 h. After 96 h, the W-TAL-AcPT1-tHMG1-IDI1 strain showed a greater extracellular accumulation of artepillin C compared to the TAL-AcPT1-tHMG1-IDI1 strain. Consequently, fed-batch cultivation with glycerol was performed using the W-TAL-AcPT1-tHMG1-IDI1 strain. As a result of the cultivation, the yeast cells increased until 96 h (OD_{600}; 350 ± 40, dry cell weight (DCW); 75 ± 8 g/L (mean ± SD), respectively) and then gradually decreased (Fig. 5A). The amount of extracellular artepillin C also increased until 96 h (5 ± 2 mg/L (mean ± SD)), after which it remained almost unchanged (Fig. 5B). The amount of intracellular artepillin C increased throughout the cultivation and reached 180 ± 20 μg/g-DCW (mean ± SD) at 144 h (Fig. 5C). Finally, the total amount of intracellular and extracellular artepillin C reached 15 ± 4 mg/L (mean ± SD) (Fig. 5D). Analyses of the intermediates *p*-CA and drupanin were also performed. There was almost no intracellular accumulation of *p*-CA after 24 h, and a transient extracellular accumulation was observed upto 48 h, which then decreased (Fig. 5BC). On the other hand, drupanin, in which *p*-CA was monoprenylated, showed almost no accumulation inside or outside the cells (Fig. 5BC). These results suggest that the supply of the prenyl donor DMAPP is sufficient in high cell density cultivation, but the supply of *p*-CA is a rate-limiting factor for the synthesis of artepillin C.

Artepillin C production by the strain with simultaneous enhancement of DMAPP and *p*-CA *in vivo* supply

As a result of the fed-batch cultivation, it was suggested that the supply of *p*-CA is the rate-limiting step in artepillin C production in the W-TAL-AcPT1-tHMG1-IDI1 strain. Therefore, to enhance the supply of *p*-CA, the *ARO4*^{K229L} and *ARO7*^{G141S} were overexpressed in W-TAL-AcPT1-tHMG1-IDI1, and the W-TAL-AcPT1-tHMG1-IDI1-ARO47m strain was constructed. The result of flask batch cultivation, as expected, the intracellular and extracellular levels of *p*-

CA increased in the W-TAL-AcPT1-tHMG1-IDI1-ARO47m strain after 24 h of cultivation (Fig. 6AD). In addition, the extracellular accumulation of drupanin and artepillin C in the culture supernatant was higher in the W-TAL-AcPT1-tHMG1-IDI1-ARO47m strain (drupanin; 22 ± 1 mg/L, and artepillin C; 2.0 ± 0.1 mg/L at 96 h) than parent strain (drupanin; 11.4 ± 0.2 mg/L, and artepillin C; 0.20 ± 0.01 mg/L at 96 h) until 96 h of cultivation (Fig. 6BC). After 96 h of cultivation, leakage of drupanin and artepillin C from the cells was observed in the parent strain, possibly due to cell lysis. As a result, the extracellular concentration of drupanin was higher in the parent strain (39 ± 1 mg/L) than in the W-TAL-AcPT1-tHMG1-IDI1-ARO47m strain (26.9 ± 0.3 mg/L), while the concentration of artepillin C was nearly the same (2.16 ± 0.03 mg/L and 2.02 ± 0.04 mg/L) at 144 h. Meanwhile, the intracellular accumulation of drupanin and artepillin C in the W-TAL-AcPT1-tHMG1-IDI1-ARO47m strain dramatically improved compared to the parent strain (Fig. 6EF). At the end of the cultivation (144 h), the amounts of drupanin and artepillin C in the W-TAL-AcPT1-tHMG1-IDI1-ARO47m strain reached 850 ± 40 μg/g-DCW and 1200 ± 100 μg/g-DCW, respectively. Notably, the intracellular accumulation of artepillin C increased approximately 10-fold compared to the maximum accumulation in the parent strain (120 ± 20 μg/g-DCW, 96 h). These results clearly indicate that simultaneously enhancing the supply of DMAPP and *p*-CA is crucial for boosting the production of artepillin C in *K. phaffii*. The total intra- and extracellular concentration of artepillin C reached 12.5 ± 0.9 mg/L, marking the highest *de novo* synthesis amount of artepillin C reported thus far, even under batch cultivation conditions.

Discussion

In this study, we have engineered the production pathway of prenylated phenylpropanoid artepillin C, which is the main bioactive component of Brazilian green propolis, in *K. phaffii* as a host organism. It should be emphasized that current supply of artepillin C through Brazilian green propolis, its main source, is unstable because the artepillin C content varies greatly due to natural factors[36], reflecting the difficulty in quality control of propolis[37]. In this context, the production of artepillin C through synthetic biology has an obvious advantage to provide this valuable compound in a stable manner. Taking the advantage of the host species *K. phaffii* that does not use the carbon flux to ethanol production and the excellent growth capability applicable to high-density culture.

In the DMAPP supply-enhanced strain developed in this study, extracellular secretion of

artepillin C was observed, while significant accumulation of artepillin C was also detected inside the cells (Fig. 4, Fig. S2). Therefore, to increase production per cultivation scale, high-density cultivation was conducted. In the fed-batch culture used in this study, approximately 20 % of the medium is diluted per 24 h due to the addition of feed solution and removal of the medium to avoid overflowing. Despite this, the amount of artepillin C in the medium increased in accordance with the rise in OD up to 96 h of cultivation (Fig. 5C). However, after 96 h, even though intracellular artepillin C increased significantly, the concentration of artepillin C in the medium remained nearly constant. This result suggests a limitation in artepillin C secretion by *K. phaffii*. Similarly, the strain with enhanced supply of both DMAPP and *p*-CA (W-TAL-AcPT1-tHMG1-IDI1-ARO47m) accumulated approximately 10 times more intracellular artepillin C than the parent strain, yet the concentration of artepillin C in the supernatant remained low (Fig. 6CF). On the other hand, drupanin, which has only one prenyl residue attached to *p*-CA, was secreted into the medium at 10 times (22 mg/L) the amount of artepillin C (Fig. 6B), suggesting that drupanin may be more easily secreted than artepillin C. The transporter involved in the efflux of artepillin C is unknown; however, in *S. cerevisiae*, for instance, some ABC transporters such as PDR5 and SNQ2 efflux more than a hundred compounds from the cells[38,39], which is beneficial if the target compounds are toxic to the host organism and are excreted from the cells. If transporters with low substrate specificity could be engineered to suppress the efflux of precursors such as *p*-CA and drupanin while promoting the efflux of artepillin C, it could be possible to increase the production yield of artepillin C.

From another perspective, to further enhance the production of artepillin C, it will be necessary to promote the two consecutive prenylation reactions from *p*-CA to artepillin C. This could be achieved through approaches such as further overexpression of prenyltransferase or enhancing the supply of DMAPP, the prenyl donor. In this study, we strengthened the supply of DMAPP by overexpressing only *IDI* and *tHMG1*. By overexpressing other MVA pathway genes or introducing mutations into ERG20 to limit carbon flux downstream of DMAPP, as done in studies with *S. cerevisiae*[8], it is expected that DMAPP supply can be further enhanced in *K. phaffii*. Recently, it has also been reported that DMAPP supply is a bottleneck in the production of the prenylated flavonoid xanthohumol in *S. cerevisiae*[40]. In this prior study, in addition to the simple enhancement of DMAPP supply through overexpression of MVA pathway genes, further production increases were achieved by fusing IDI with prenyltransferase. Therefore, in the production of artepillin C, it is also possible that the fusion of IDI and AcPT1 could efficiently utilize DMAPP in the prenylation reaction.

In the fields of synthetic biology and metabolic engineering, plant metabolites are often chosen as targets[41] due to their beneficial chemical properties, including flavor, pigments, sweetness, UV protection, and medicinal properties[42]. These metabolites are broadly categorized into three groups: phenolic compounds, isoprenoids, and alkaloids. Some of these compounds have been successfully produced in microorganisms. For example, thebaine, a type of alkaloid, was produced in yeast by introducing over 20 genes from various organisms, achieving a concentration of 6.4 μg/L[43]. Noscapine, an alkaloid used as a cough suppressant, was also synthesized in yeast, with production reaching 2.2 mg/L through the expression of over 30 biosynthetic genes from different species[44]. A notable synthetic biology achievement is the production of artemisinin, a potent antimalarial drug, through the engineering of yeast to synthesize 25 g/L of artemisinic acid, its chemical precursor[45]. Artemisinic acid belongs to the class of isoprenoid compounds.

Compared to the above reports, synthetic biology using membrane-bound PTs is still rare. Icariin, a prenylated kaempferol derivative, was synthesized *de novo* in yeast using a kaempferol-specific PT[6]. As another example, the complete biosynthesis of cannabinoids including cannabigerolic acid was also achieved in yeast, in which a new geranyltransferase for olivetolic acid was cloned and introduced[7]. These reports indicate that the identification of a PT specifically involved in the target compound is the key to success. Bacteria and fungi have PTs of the soluble type[46]. These enzymes are less problematic to express in microorganisms, whereas these enzymes generally have broad substrate specificities and thus a risk of producing unwanted by-products when applied in synthetic biology. For the production of the target compound, plant-derived PTs still have an advantage as they generally show sharp specificities for both substrate and product.

In this study, we have successfully enforced both pathways to provide the phenylpropanoid acceptor substrate (*p*-CA) and the isoprenoid donor substrate (DMAPP). For prenylated phenolic compounds, most aromatic cores are biosynthesized via *p*-CA and most prenyl moiety found in nature is dimethylallyl residue, suggesting that the strains established in this study will be applicable for the production of many other divergent prenylated phenolic substances, as well.

Methods

Strains and media

The NovaBlue strain of *E. coli* (Merck Millipore, Darmstadt, Germany) was used for plasmid construction and amplification. NovaBlue was routinely grown in LB medium (10 g/L tryptone, 5 g/ L yeast extract, and 5 g/L NaCl) containing 100 μg/mL ampicillin at 37 °C. The yeast strains used in this study are listed in Table 1. *K. phaffii* CBS7435 and *K. phaffii* CBS7435*Δdnl4Δhis4*[47] were used as the yeast host strain. *K. phaffii* strains were routinely grown in YPD medium (10 g/L yeast extract, 20 g/L peptone, and 20 g/L glucose) supplemented with appropriate antibiotics (500 μ g/mL G418, 300 μ g/mL hygromycin, and 100 μ g/mL Zeocin).

Plasmids construction

Table 2 and Table S1 show all plasmids and primers used in this study, respectively. All plasmids were constructed by using the In-fusion HD cloning kit (Takara Bio USA, Mountain View, CA, USA) according to the manufacturer's instructions. *AcPT1* was codon-optimized for *K. phaffii* and synthesized by GeneArt (Thermo Fisher Scientific, Waltham, MA, USA).

The AcPT1 integrative plasmids (pPGPZ-PT1 and pPGPZ-tTP_PT1) were constructed as follows: The DNA fragment encoding *AcPT1* was amplified from the synthetic gene by polymerase chain reaction (PCR) using the AcPT1-F and AcPT1-R primers. The TP-truncated sequence (tTP_AcPT1) was also amplified from the synthetic gene by PCR using the tTP_AcPT1-F and AcPT1-R primers. The *AcPT1* and *tTP_AcPT1* fragments were inserted into the pPGPZ-EGFP vector, which was double digested with SpeI and XhoI[23] to generate plasmids pPGPZ-AcPT1 and pPGPZ-tTP_AcPT1, respectively. The integrative plasmids for *TAL* and *AcPT1* (pPGP-TAL-AcPT1 and pPGP-TAL-tTP_AcPT1) were constructed as follows: The *GAP* promoter (P_{gap})-AcPT1-*GAP* terminator (T_{gap}) and P_{gap}-tTP_AcPT1-T_{gap} fragments were amplified from pPGPZ-AcPT1 and pPGPZ-tTP_AcPT1 using the 112-AatⅡ-F and 112-AatII-R primers by PCR. The P_{gap}-AcPT1-T_{gap} and P_{gap}-tTP_AcPT1-T_{gap} fragments were cloned into AatII-digested pPGP-TAL[23] to generate plasmids pPGP-TAL-AcPT1 and pPGP-TAL-tTP_AcPT1, respectively. The *S. cerevisiae tHMG1*-integrative plasmids

(pPGPZ-tHMG1) were constructed as follows: The DNA fragment encoding tHMG1 was amplified from genomic DNA of *S. cerevisiae* YPH499 (Stratagene, La Jolla, CA, USA) by PCR using the tHMG1-F and tHMG1-R primers. The *tHMG1* fragment was cloned into the pPGPZ-EGFP vector using SpeI and XhoI sites to generate plasmid pPGPZ-tHMG1. The integrative plasmids for *TAL*, *AcPT1*, and *tHMG1* (pPGP-TAL-AcPT1-tHMG1) were constructed as follows: The P_{gap}-tHMG1-T_{gap} fragment was amplified from pPGPZ-tHMG1 by PCR using the 112-BstAPI-F and 112-BstAPI-R primers. The P_{gap}-tHMG1-T_{gap} fragment was cloned into BstAPI digested pPGP-TAL-AcPT1 vector to generate plasmid pPGP-TAL-AcPT1-tHMG1. The *IDI1*-integrative plasmids (pPGPZ-IDI1) were constructed as follows: The DNA fragment encoding *IDI1* was amplified from *K. phaffii* CBS7435 genome DNA by PCR using the IDI1-F and IDI1-R primers. The *IDI1* fragment was cloned into the pPGPZ-EGFP vector using SpeI and XhoI sites to generate plasmid pPGPZ-IDI1. The integrative plasmid for *tHMG1* and *IDI1* (pPGPZ-tHMG1-IDI1) was constructed as follows: The P_{gap}-tHMG1-T_{gap} fragment was amplified from pPGPZ-tHMG1 by PCR using the 141-SphI-F and 141-SphI-R primers. The P_{gap}-tHMG1-T_{gap} fragment was cloned into the SphI-digested pPGPZ-IDI1 vector to generate plasmid pPGPZ-tHMG1-IDI1.

Yeast transformation

Transformation of *K. phaffii* was performed by the lithium acetate method[35]. The resulting transformants were selected on YPD agar plates supplemented with appropriate antibiotics (500 μg/mL G418, 300 μg/mL hygromycin, 100 μg/mL Zeocin). The *TAL* overexpression strain (TAL) was constructed as follows: The pPGP-TAL plasmid was linearized with EcoRV, transfected into the CBS7435 *Δdnl4 Δhis4* strain, and integrated into the genomic DNA by single crossover recombination, yielding the TAL strain. The strains co-overexpressing *TAL* and *AcPT1* (TAL-AcPT1 and TAL-tTP_AcPT1) were constructed as follows: The pPGP-TAL-AcPT1 and pPGP-TAL-tTP_AcPT1 plasmids were linearized with EcoRV, transfected into the CBS7435 *Δdnl4 Δhis4* strain, and integrated into the genomic DNA by single crossover recombination, resulting in the TAL-AcPT1 and TAL-tTP_AcPT1 strains. The *TAL*, *AcPT1*, *ARO4*^{K229L}, and *ARO7*^{G141S} co-overexpression strain (TAL-AcPT1-ARO47m) was constructed as follows: The pPGPH-ARO4^{K229L}-ARO7^{G141S} plasmid was linearized with BsrGI, transfected into the TAL-AcPT1 strain, and integrated into the genomic DNA by single crossover recombination, resulting in TAL-AcPT1-ARO47m strain. The strain co-overexpressing *TAL*,

AcPT1, and *tHMG1* (TAL-AcPT1-tHMG1) was constructed as follows: The pPGP-TAL-AcPT1-tHMG1 plasmid was linearized with EcoRV, transfected into the CBS7435 *Δdnl4 Δhis4* strain, and integrated in the genomic DNA by single crossover recombination, resulting in the TAL-AcPT1-tHMG1 strain. The strain co-overexpressing *TAL*, *AcPT1*, and *IDI1* (TAL-AcPT1-IDI1) was constructed as follows: pPGPZ-IDI1 plasmid was linearized with PmeI, transfected into the TAL-AcPT1 strain, and integrated in the genomic DNA by single crossover recombination, yielding the TAL-AcPT1-IDI1 strain. The strains co-overexpressing *TAL*, *AcPT1*, *tHMG1* and *IDI1* (TAL-AcPT1-tHMG1-IDI1 and W-TAL-AcPT1-tHMG1-IDI1) were constructed as follows: pPGPZ-tHMG1-IDI1 plasmid was linearized with PmeI, transfected into the TAL-AcPT1 strain, and integrated into the genomic DNA by single crossover recombination, yielding TAL-AcPT1-tHMG1-IDI1 strain. W-TAL-AcPT1-tHMG1-IDI1 was also constructed using CBS7435 WT as the parent strain using the same procedure. The strain co-overexpressing *TAL*, *AcPT1*, *IDI1, ARO4*^{K229L}, and *ARO7*^{G141S} (W-TAL-AcPT1-IDI1-ARO47m) was constructed as follows: The pPGPH-ARO4^{K229L}-ARO7^{G141S} plasmid was linearized with BsrGI, transfected into the W-TAL-AcPT1-IDI1 strain, and integrated into the genomic DNA by single crossover recombination, resulting in W-TAL-AcPT1-IDI1-ARO47m strain.

Batch fermentation in the flask

For the pre-cultivation, yeast cells were inoculated into 5 mL of YPG [10 g/L yeast extract, 20 g/L peptone (BD Biosciences, San Jose, CA), and 20 g/L glycerol] medium supplemented with appropriate antibiotics in test tubes and cultured at 30 °C and 200 rpm. After overnight cultivation, the cells were harvested by centrifugation at 15,000g for 1 minute, and washed twice with sterile water. Yeast cells were inoculated into 20 mL of YPG medium in 100-mL baffled flasks at an initial OD_{600} of 0.05, and cultured at 30 °C and 150 rpm in an orbital shaker incubator (BR-43FL; Taitec, Saitama, Japan).

Fed-batch fermentation in the jar fermentor

Yeast cells were precultured in 20 mL of BMGY medium [10 g/L yeast extract, 20 g/L hipolypepton NS (FUJIFILM Wako Pure Chemical, OSAKA, Japan), 13.4 g/L yeast nitrogen base without amino acids (Difco Laboratories, Detroit, MI, USA), 0.4 mg/L biotin, 50 mM

potassium phosphate buffer (pH 5.5), 50 mM ammonium phosphate buffer (pH 5.5), and 20 g/L glycerol] in a 100-mL Erlenmeyer flask at 30 °C and 150 rpm for 24 h. After pre-cultivation, the yeast cells were inoculated a 250-mL jar fermentor (Bio Jr., 8; ABLE Biott, Tokyo, Japan) with an initial OD_{600} of 0.05. Fermentation was performed at 30 °C and the air flow was maintained at 150 mL/min. The agitation speed was maintained at 900 rpm. The pH of the culture medium was maintained at 6.0 by the automatic addition of a 5 N ammonium hydroxide. The antifoam SI (FUJIFILM Wako Pure Chemical) was added at the appropriate time when foaming occurred. After 24 h cultivation, 0.5 mL feeding solution [10 g/L yeast extract, 20 g/L hipolypepton NS (FUJIFILM Wako Pure Chemical), 13.4 g/L yeast nitrogen base without amino acids (Difco Laboratories), 0.4 mg/L biotin, 50 mM potassium phosphate buffer (pH 5.5), 50 mM ammonium phosphate buffer (pH 5.5), and 500 g/L glycerol] was added every 30 minutes using a peristaltic pump. After 48 hours of cultivation, 25 mL of the samples were taken every 24 hours to measure the OD_{600}, dry cell weight, and metabolite concentrations.

Extraction of metabolites from yeast cells

Yeast cells were harvested by centrifugation at 13,000 rpm for 3 minutes at 4 °C. The pellet was washed twice with 500 µL distilled water and suspended in 375 µL ethyl acetate containing 50 µL 3M HCl. The suspended cells were mixed with 200 µL glass beads (0.1-mm diameter), disrupted by shaking at 1500 rpm for 15 minutes using a Shake Master Neo (Biomedical Science, Tokyo, Japan), and centrifuged at 15,000 rpm and 4 °C for 15 minutes. The 150 µL supernatant was collected as the cell extract and dried under vacuum using a Free Zone 2.5 Plus system (Labconco, Kansas City, MO, USA). Dried metabolites were dissolved in 50 µL of 99.5 % ethanol prior to analysis.

Analytical methods

The glycerol concentration in the medium was analyzed using high-performance liquid chromatography (HPLC) (Shimadzu, Kyoto, Japan). Details of the method have been reported previously[23]. The concentrations of *p*-CA and artepillin C were analyzed by HPLC equipped with a Luna Omega PS C18 column (4.6 × 150 mm2, 3 µm particle size; Phenomenex, CA) and UV detector. Details of the method have been reported previously[48].

467

Table 1 Strains used in this study

strains	Description	Source
K. phaffii CBS7435	CBS7435 (ATCC 76273)	ATCC*
CBS7435 Δ*dnl4* Δ*his4*	*Δdnl4Δhis4*::*ADE1*	(35)
TAL	CBS7435*Δdnl4Δhis4*/pPGP-TAL	(23)
TAL-AcPT1	CBS7435*Δdnl4Δhis4*/pPGP-TAL-AcPT1	This study
TAL-tTP_AcPT1	CBS7435*Δdnl4Δhis4*/pPGP-TAL-tTP_AcPT1	This study
TAL-AcPT1-ARO47m	TAL-PT1/pPGPH-ARO4^{K229L}-ARO7^{G141S}	This study
TAL-AcPT1-tHMG1	CBS7435*Δdnl4Δhis4*/pPGP-TAL-AcPT1-tHMG1	This study
TAL-AcPT1-IDI1	TAL-AcPT1/pPGPZ-IDI1	This study
TAL-AcPT1-tHMG1-IDI1	TAL-AcPT1/pPGPZ-tHMG1-IDI1	This study
W-TAL-AcPT1-tHMG1-IDI1	CBS7435/pPGP-TAL-AcPT1/pPGPZ-tHMG1-IDI1	This study
W-TAL-AcPT1-tHMG1-IDI1-ARO47m	CBS7435/pPGP-TAL-AcPT1/pPGPZ-tHMG1-IDI1/pPGPH-ARO4^{K229L}-ARO7^{G141S}	This study

* ATCC, American Type Culture Collection.

Table 2 Plasmids used in this study

plasmids	Description	Source
pPGP-EGFP	P_{gap}-*EGFP*-T_{aox1}, *G418* marker	(47)
pPGPZ-EGFP	P_{gap}-*EGFP*-T_{aox1}, *Zeo* marker	(23)
pPGP-TAL	P_{gap}-*HaTAL*-T_{aox1}, *G418* marker	(23)
pPGPZ-AcPT1	P_{gap}-*AcPT1*-T_{aox1}, *Zeo* marker	This study
pPGPZ-tTP_AcPT1	P_{gap}-*tTP_AcPT1*-T_{aox1}, *Zeo* marker	This study
pPGP-TAL-AcPT1	P_{gap}-*HaTAL*-T_{aox1}, P_{gap}-*AcPT1*-T_{aox1}, *G418* marker	This study
pPGP-TAL-tTP_AcPT1	P_{gap}-*HaTAL*-T_{aox1}, P_{gap}-*tTP_AcPT1*-T_{aox1}, *G418* marker	This study
pPGPH-ARO4^{K229L}-ARO7^{G141S}	P_{gap}-*ARO4*^{K229L}-T_{aox1}, P_{gap}-*ARO7*^{G141S}-T_{aox1}, *Hyg* marker	(23)
pPGPZ-tHMG1	P_{gap}-*tHMG1*-T_{aox1}, *Zeo* marker	This study
pPGP-TAL-PT1-tHMG1	P_{gap}-*HaTAL*-T_{aox1}, P_{gap}-*tTP_AcPT1*-T_{aox1}, P_{gap}-*tHMG1*-T_{aox1}, *G418* marker	This study

pPGPZ-IDI1	P_{gap}-*PpIDI1*-T_{aox1}, *Zeo* marker	This study
pPGPZ-tHMG1-IDI1	P_{gap}-*tHMG1*-T_{aox1}, P_{gap}-*PpIDI1*-T_{aox1}, *Zeo* marker	This study

Figure legends

Figure 1. The biosynthetic pathway of artepillin C in *K. phaffii.*

Solid arrows indicate single reaction steps and the dashed arrows indicate multiple enzymatic steps. Abbreviations for metabolites and enzymes: PEP, phosphoenolpyruvate; E4P, erythrose 4-phosphate; DAHP, 3-deoxy-D-arabinoheptulosonate 7-phosphate; HMG-CoA, 3-hydroxy-3-methylglutaryl coenzyme A; IPP, isopentenyl pyrophosphate; DMAPP, dimethylallyl pyrophosphate; $ARO4^{K299L}$, a DAHP synthase mutant (K229L) from *S. cerevisiae*; $ARO7^{G141S}$, a chorismate mutase mutant (G141S) from *S. cerevisiae*; TAL, a tyrosine ammonia-lyase from *Herpetosiphon aurantiacus*; AcPT1, *Artemisia capillaris* prenyltransferase 1; tHMG1, an N-terminal truncated hydroxy-3-methylglutaryl coenzyme A reductase from *S. cerevisiae*; IDI1, an isopentenyl diphosphate delta isomerase from *K. phaffii.*

Figure 2. Engineering of *K. phaffii* expressing *TAL*.

(A) Ratio of intracellular and extracellular *p*-CA levels after 96 h of cultivation of *K. phaffii* strains overexpressing *TAL* in YPG medium. (B) Time course of intracellular artepillin C levels in YPG medium of engineered strains (TAL-AcPT1 and TAL-tTP_AcPT1) and a control strain (CBS7435*Δdnl4Δhis4*). All results are expressed as mean ± standard deviation of three biologically independent experiments.

Figure 3. Artepillin C production by a *K. phaffii* strain overexpressing $ARO4^{K299L}$ and $ARO7^{G141S}$ (TAL-AcPT1-ARO47).

Time course of artepillin C (solid lines) and *p*-CA (dashed lines) production levels in the cell fraction (A) and the medium fraction (B). Cell growth (solid lines) and glycerol consumption (dashed lines) are shown in (C). Results are presented as mean ± standard deviation of three biologically independent experiments.

Figure 4. Artepillin C production by *K. phaffii* strains with enhanced DMAPP supply.

TAL-AcPT1-tHMG1, TAL-AcPT1-IDI1, and TAL-AcPT1-tHMG1-IDI1 were overexpressed in *K. phaffii*. Time courses of artepillin C production in the cell fraction (A) and that in the

medium fraction (B). Results are presented as mean ± standard deviation of three biologically independent experiments.

Figure 5. Fed-batch cultivation of the W-TAL-AcPT1-tHMG1-IDI1 strain with glycerol.

Time course monitoring of (A) OD_{600} and dry cell weight (DCW), (B) intracellular metabolites, (C) extracellular metabolites, and (D) the total artepillin C level. Results are presented as mean ± standard deviation of three biologically independent experiments.

Figure 6. Artepillin C production by *K. phaffii* strains with enhanced DMAPP and *p*-CA *in vivo* supply.

Time course of intracellular amounts of (A) *p*-CA, (B) drupanin, and (C) artepillin C, and extracellular amounts of (D) *p*-CA, (E) drupanin, and (F) artepillin C. Results are presented as mean ± standard deviation of three biologically independent experiments.

Supporting Information Contents

Fig. S1 Growth curves of CBS7435WT and CBS7435 Δdnl4 Δhis4 in glycerol fed-batch cultivation.

Fig. S2 Flask batch cultivation of the TAL-AcPT1-tHMG1-IDI1 and W-TAL-AcPT1-tHMG1-IDI1 strain.

Tabale S1 Primers used in this study

Acknowledgements

This work was financially supported by Grant-in-Aid for Transformative Research Areas (A) from the Japan Society for the Promotion of Science (JSPS, grant No. 23H04967 to R.M. and K.Y.) and RIKEN Cluster for Science, Technology and Innovation Hub (RCSTI to K.Y.). This

research was also supported by the Program for Forming Japan's Peak Research Universities (J-PEAKS) from JSPS, and the GteX Program Japan from Japan Science and Technology Agency (JST, grant No. JPMJGX23B4). Drupanin standard was kindly provided by Yamada Bee Company, Inc. We also thank Dr. Futoshi Taura (Iwate Medical University) and Dr. Hirobumi Yamamoto (Toyo University) for providing technical advice and a standard specimen, respectively.

Author information

Corresponding authors

Kazufumi Yazaki - Laboratory of Plant Gene Expression, Research Institute for Sustainable Humanosphere, Kyoto University, Uji 611–0011, Japan; orcid.org/0000-0003-2523-6418; Email; yazaki@rish.kyoto-u.ac.jp

Tomohisa Hasunuma - Engineering Biology Research Center, Kobe University, Nada, Kobe 657-8501, Japan; Graduate School of Science, Technology and Innovation, Kobe University, Nada, Kobe 657-8501, Japan; Biomass Engineering Program, RIKEN, Yokohama, Kanagawa 230-0045, Japan; orcid.org/0000-0002-8382-2362; Email: hasunuma@port.kobe-u.ac.jp;

Authors

Takahiro Bamba - Engineering Biology Research Center, Kobe University, 1-1 Rokkodai, Nada, Kobe, 657-8501, Japan

Ryosuke Munakata - Laboratory of Plant Gene Expression, Research Institute for Sustainable Humanosphere, Kyoto University, Uji 611–0011, Japan

Yuya Ushiro - Graduate School of Science, Technology, and Innovation, Kobe University, 1-1 Rokkodai, Nada, Kobe, 657-8501, Japan

Ryota Kumokita - Graduate School of Science, Technology, and Innovation, Kobe University, 1-1 Rokkodai, Nada, Kobe, 657-8501, Japan

Sayaka Tanaka - Graduate School of Science, Technology, and Innovation, Kobe University, 1-1 Rokkodai, Nada, Kobe, 657-8501, Japan

Yoshimi Hori - Engineering Biology Research Center, Kobe University, 1-1 Rokkodai, Nada,

Kobe, 657-8501, Japan

Akihiko Kondo - Engineering Biology Research Center, Kobe University, Nada, Kobe 657-8501, Japan; Graduate School of Science, Technology and Innovation, Kobe University, Nada, Kobe 657-8501, Japan; Biomass Engineering Program, RIKEN, Yokohama, Kanagawa 230-0045, Japan; orcid.org/0000-0003-1527-5288

Author contributions

R.M., K.Y., and T.H. designed the experiments. T.B., R.M., Y.U., R.K., S.T., and Y.H. performed the experiments. All authors discussed the results. T.B., K.Y., and T.H. wrote the manuscript. R.M., K.Y., A.K., and T.H. supervised all aspects of the study.

References

(1) Munakata, R.; Yazaki, K. How Did Plants Evolve the Prenylation of Specialized Phenolic Metabolites by Means of UbiA Prenyltransferases? *Curr. Opin. Plant Biol.* **2024**, *81*, 102601.

(2) Mukai, R.; Horikawa, H.; Fujikura, Y.; Kawamura, T.; Nemoto, H.; Nikawa, T.; Terao, J. Prevention of Disuse Muscle Atrophy by Dietary Ingestion of 8-Prenylnaringenin in Denervated Mice. *PLoS One* **2012**, *7*(9), e45048.

(3) Murakami, A.; Kuki, W.; Takahashi, Y.; Yonei, H.; Nakamura, Y.; Ohto, Y.; Ohigashi, H.; Koshimizu, K. Auraptene, a Citrus Coumarin, Inhibits 12-*O*-Tetradecanoylphorbol-13-acetate-induced Tumor Promotion in ICR Mouse Skin, Possibly through Suppression of Superoxide Generation in Leukocytes. *Jpn. J. Cancer Res.* **1997**, *88* (5), 443–452.

(4) Cervo, L.; Rozio, M.; C., E.-S.; Guiso, G.; Morazzoni, P.; Caccia, S. Role of Hyperforin in the Antidepressant-like Activity of *Hypericum perforatum* Extracts. *Psychopharmacology* **2002**, *164* (4), 423–428.

(5) Berenbaum, M.; Feeny, P. Toxicity of Angular Furanocoumarins to Swallowtail Butterflies: Escalation in a Coevolutionary Arms Race? *Science* **1981**, *212* (4497), 927–929.

(6) An, T.; Lin, G.; Liu, Y.; Qin, L.; Xu, Y.; Feng, X.; Li, C. *De Novo* Biosynthesis of Anticarcinogenic Icariin in Engineered Yeast. *Met. Eng.* **2023**, *80*, 207–215.

(7) Luo, X.; Reiter, M. A.; d'Espaux, L.; Wong, J.; Denby, C. M.; Lechner, A.; Zhang, Y.; Grzybowski, A. T.; Harth, S.; Lin, W.;Lee, H.; Yu, C.; Shin, J.; Deng, K.; Benites, V. T.; Wang, G.; Baidoo, E. E. K.; Chen, Y.; Dev, I.; Petzold, C. J.; Keasling, J. D. Complete

Biosynthesis of Cannabinoids and Their Unnatural Analogues in Yeast. *Nature* **2019**, *567* (7746), 123–126.

(8) Ding, Y.; Ning, Y.; Xin, D.; Fu, Y. Dual Cytoplasmic-peroxisomal Compartmentalization Engineering and Multiple Metabolic Engineering Strategies for High Yield Non-psychoactive Cannabinoid in *Saccharomyces cerevisiae*. *Biotechnol. J.* **2024**, *19* (2), 2300590.

(9) Cheng, W.; Li, W. Structural Insights into Ubiquinone Biosynthesis in Membranes. *Science* **2014**, *343* (6173), 878–881.

(10) Aga, H.; Shibuya, T.; Sugimoto, T.; Kurimoto, M.; Nakajima, S. Isolation and Identification of Antimicrobial Compounds in Brazilian Propolis. *Biosci. Biotechnol. Biochem.* **1994**, *58* (5), 945–946.

(11) Zhang, C.; Shen, X.; Chen, J.; Jiang, X.; Hu, F. Identification of Free Radical Scavengers from Brazilian Green Propolis Using Off-Line HPLC-DPPH Assay and LC-MS. *J. Food Sci.* **2017**, *82* (7), 1602–1607.

(12) Paulino, N.; Abreu, S. R. L.; Uto, Y.; Koyama, D.; Nagasawa, H.; Hori, H.; Dirsch, V. M.; Vollmar, A. M.; Scremin, A.; Bretz, W. A. Anti-Inflammatory Effects of a Bioavailable Compound, Artepillin C, in Brazilian Propolis. *Eur. J. Pharmacol.* **2008**, *587* (1–3), 296–301.

(13) Chan, G. C.-F.; Cheung, K.-W.; Sze, D. M.-Y. The Immunomodulatory and Anticancer Properties of Propolis. *Clinic. Rev. Allerg. Immunol.* **2013**, *44* (3), 262–273.

(14) Kimoto, T.; Koya-Miyata, S.; Hino, K.; Micallef, M.; Hanaya, T.; Arai, S.; Ikeda, M.; Kurimoto, M. Pulmonary Carcinogenesis Induced by Ferric Nitrilotriacetate in Mice and Protection from It by Brazilian Propolis and Artepillin C. *Virchows Arch.* **2001**, *438* (3), 259–270.

(15) Shimizu, K.; Das, S. K.; Baba, M.; Matsuura, Y.; Kanazawa, K. Dietary Artepillin C Suppresses the Formation of Aberrant Crypt Foci Induced by Azoxymethane in Mouse Colon. *Cancer Lett.* **2006**, *240* (1), 135–142.

(16) Nishikawa, S.; Aoyama, H.; Kamiya, M.; Higuchi, J.; Kato, A.; Soga, M.; Kawai, T.; Yoshimura, K.; Kumazawa, S.; Tsuda, T. Artepillin C, a Typical Brazilian Propolis-Derived Component, Induces Brown-like Adipocyte Formation in C3H10T1/2 Cells, Primary Inguinal White Adipose Tissue-Derived Adipocytes, and Mice. *PLoS One* **2016**, *11* (9), e0162512.

(17) Kumazawa, S.; Yoneda, M.; Shibata, I.; Kanaeda, J.; Hamasaka, T.; Nakayama, T. Direct Evidence for the Plant Origin of Brazilian Propolis by the Observation of Honeybee Behavior and Phytochemical Analysis. *Chem. Pharm. Bull.* **2003**, *51* (6), 740–742.

(18) Gazim, Z. C.; Valle, J. S.; Carvalho dos Santos, I.; Rahal, I. L.; Silva, G. C. C.; Lopes, A.

D.; Ruiz, S. P.; Faria, M. G. I.; Piau Junior, R.; Gonçalves, D. D. Ethnomedicinal, Phytochemical and Pharmacological Investigations of *Baccharis dracunculifolia* DC. (ASTERACEAE). *Front. Pharmacol.* **2022**, *13*, 1048688.

(19) Munakata, R.; Takemura, T.; Tatsumi, K.; Moriyoshi, E.; Yanagihara, K.; Sugiyama, A.; Suzuki, H.; Seki, H.; Muranaka, T.; Kawano, N.; Yoshimatsu, K.; Kawahara, N.; Yamaura, T.; Grosjean, J.; Bourgaud, F.; Hehn, A.; Yazaki, K. Isolation of *Artemisia capillaris* Membrane-Bound Di-Prenyltransferase for Phenylpropanoids and Redesign of Artepillin C in Yeast. *Commun. Biol.* **2019**, *2* (1), 384.

(20) Patra, P.; Das, M.; Kundu, P.; Ghosh, A. Recent Advances in Systems and Synthetic Biology Approaches for Developing Novel Cell-Factories in Non-Conventional Yeasts. *Biotechnol. Adv.* **2021**, *47*, 107695.

(21) Karbalaei, M.; Rezaee, S. A.; Farsiani, H. *Pichia pastoris*: A Highly Successful Expression System for Optimal Synthesis of Heterologous Proteins. *J. Cellular Physiol.* **2020**, *235* (9), 5867–5881.

(22) Bhattacharya, S.; Esquivel, B. D.; White, T. C. Overexpression or Deletion of Ergosterol Biosynthesis Genes Alters Doubling Time, Response to Stress Agents, and Drug Susceptibility in *Saccharomyces cerevisiae*. *mBio* **2018**, *9* (4), e01291-18.

(23) Kumokita, R.; Bamba, T.; Inokuma, K.; Yoshida, T.; Ito, Y.; Kondo, A.; Hasunuma, T. Construction of an L-Tyrosine Chassis in *Pichia pastoris* Enhances Aromatic Secondary Metabolite Production from Glycerol. *ACS Synth. Biol.* **2022**, *11* (6), 2098–2107.

(24) Liu, W.-C.; Inwood, S.; Gong, T.; Sharma, A.; Yu, L.-Y.; Zhu, P. Fed-Batch High-Cell-Density Fermentation Strategies for *Pichia pastoris* Growth and Production. *Crit. Rev. Biotechnol.* **2019**, *39* (2), 258–271.

(25) Looser, V.; Bruhlmann, B.; Bumbak, F.; Stenger, C.; Costa, M.; Camattari, A.; Fotiadis, D.; Kovar, K. Cultivation Strategies to Enhance Productivity of *Pichia pastoris*: A Review. *Biotechnol. Adv.* **2015**, *33* (6), 1177–1193.

(26) Shen, G.; Huhman, D.; Lei, Z.; Snyder, J.; Sumner, L. W.; Dixon, R. A. Characterization of an Isoflavonoid-Specific Prenyltransferase from *Lupinus albus*. *Plant Physiol.* **2012**, *159* (1), 70–80.

(27) Munakata, R.; Inoue, T.; Koeduka, T.; Karamat, F.; Olry, A.; Sugiyama, A.; Takanashi, K.; Dugrand, A.; Froelicher, Y.; Tanaka, R.; Uto, Y.; Hori, H.; Azuma, J-I.; Hehn, A.; Bourgaud, F.; Yazaki, K. Molecular Cloning and Characterization of a Geranyl Diphosphate-Specific Aromatic Prenyltransferase from Lemon. *Plant Physiol.* **2014**, *166* (1), 80–90.

(28) Kumokita, R.; Yoshida, T.; Shirai, T.; Kondo, A.; Hasunuma, T. Aromatic Secondary Metabolite Production from Glycerol Was Enhanced by Amino Acid Addition in *Pichia*

Pastoris. Appl. Microbiol. Biotechnol. **2023**, *107* (24), 7391–7401.

(29) Gottardi, M.; Reifenrath, M.; Boles, E.; Tripp, J. Pathway Engineering for the Production of Heterologous Aromatic Chemicals and Their Derivatives in *Saccharomyces cerevisiae*: Bioconversion from Glucose. *FEMS Yeast Res.* **2017**, *17* (4), fox035.

(30) Suástegui, M.; Shao, Z. Yeast Factories for the Production of Aromatic Compounds: From Building Blocks to Plant Secondary Metabolites. *J. Ind. Microbiol. Biotechnol.* **2016**, *43* (11), 1611–1624.

(31) Chen, R.; Gao, J.; Yu, W.; Chen, X.; Zhai, X.; Chen, Y.; Zhang, L.; Zhou, Y. J. Engineering Cofactor Supply and Recycling to Drive Phenolic Acid Biosynthesis in Yeast. *Nature Chem. Biol.* **2022**, *18* (5), 520–529.

(32) Shimazaki, S.; Yamada, R.; Yamamoto, Y.; Matsumoto, T.; Ogino, H. Building a Machine-learning Model to Predict Optimal Mevalonate Pathway Gene Expression Levels for Efficient Production of a Carotenoid in Yeast. *Biotechnol. J.* **2024**, *19* (1), 2300285.

(33) Kirby, J.; Romanini, D. W.; Paradise, E. M.; Keasling, J. D. Engineering Triterpene Production in *Saccharomyces cerevisiae* – β -Amyrin Synthase from *Artemisia annua*. *FEBS J.* **2008**, *275* (8), 1852–1859.

(34) Yao, Z.; Zhou, P.; Su, B.; Su, S.; Ye, L.; Yu, H. Enhanced Isoprene Production by Reconstruction of Metabolic Balance between Strengthened Precursor Supply and Improved Isoprene Synthase in *Saccharomyces cerevisiae*. *ACS Synth. Biol.* **2018**, *7* (9), 2308–2316.

(35) Ito, Y.; Watanabe, T.; Aikawa, S.; Nishi, T.; Nishiyama, T.; Nakamura, Y.; Hasunuma, T.; Okubo, Y.; Ishii, J.; Kondo, A. Deletion of DNA Ligase IV Homolog Confers Higher Gene Targeting Efficiency on Homologous Recombination in *Komagataella phaffii*. *FEMS Yeast Res.* **2018**, *18* (7), foy074.

(36) Jorge, R.; Furtado, N. A. J. C.; Sousa, J. P. B.; Da Silva Filho, A. A.; Gregório Junior, L. E.; Martins, C. H. G.; Soares, A. E. E.; Bastos, J. K.; Cunha, W. R.; Silva, M. L. A. Brazilian Propolis: Seasonal Variation of the Prenylated *p* -Coumaric Acids and Antimicrobial Activity. *Pharm. Biol.* **2008**, *46* (12), 889–893.

(37) Toreti, V. C.; Sato, H. H.; Pastore, G. M.; Park, Y. K. Recent Progress of Propolis for Its Biological and Chemical Compositions and Its Botanical Origin. *Evid.Based Complement. Alternat. Med.* **2013**, *2013*, 1–13.

(38) Hirata, D.; Yano, K.; Miyahara, K.; Miyakawa, T. *Saccharomyces cerevisiae YDR1*, Which Encodes a Member of the ATP-Binding Cassette (ABC) Superfamily, Is Required for Multidrug Resistance. *Curr. Genet.* **1994**, *26* (4), 285–294.

(39) Servos, J.; Haase, E.; Brendel, M. Gene *SNQ2* of *Saccharomyces cerevislae*, Which

Confers Resistance to 4-Nitroquinoline-N-Oxide and Other Chemicals, Encodes a 169 kDa Protein Homologous to ATP-Dependent Permeases. *Mol. Gen. Genet.* **1993**, *236–236* (2–3), 214–218.

(40) Yang, S.; Chen, R.; Cao, X.; Wang, G.; Zhou, Y. J. *De Novo* Biosynthesis of the Hops Bioactive Flavonoid Xanthohumol in Yeast. *Nature Commun.* **2024**, *15* (1), 253.

(41) Afendi, F. M.; Okada, T.; Yamazaki, M.; Hirai-Morita, A.; Nakamura, Y.; Nakamura, K.; Ikeda, S.; Takahashi, H.; Altaf-Ul-Amin, M.; Darusman, L. K.; Saito, K.; Kanaya, S. KNApSAcK Family Databases: Integrated Metabolite–Plant Species Databases for Multifaceted Plant Research. *Plant Cell Physiol.* **2012**, *53* (2), e1.

(42) Rai, A.; Saito, K.; Yamazaki, M. Integrated Omics Analysis of Specialized Metabolism in Medicinal Plants. *Plant J.* **2017**, *90* (4), 764–787.

(43) Galanie, S.; Thodey, K.; Trenchard, I. J.; Filsinger Interrante, M.; Smolke, C. D. Complete Biosynthesis of Opioids in Yeast. *Science* **2015**, *349* (6252), 1095–1100.

(44) Li, Y.; Li, S.; Thodey, K.; Trenchard, I.; Cravens, A.; Smolke, C. D. Complete Biosynthesis of Noscapine and Halogenated Alkaloids in Yeast. *Proc. Natl. Acad. Sci. U.S.A.* **2018**, *115* (17).

(45) Paddon, C. J.; Westfall, P. J.; Pitera, D. J.; Benjamin, K.; Fisher, K.; McPhee, D.; Leavell, M. D.; Tai, A.; Main, A.; Eng, D. Polichuk, D. R.; Teoh, K. H.; Reed, D. W.; Treynor, T.; Lenihan, J.; Jiang, H.; Fleck, M.; Bajad, S.; Dang, G.; Dengrove, D.; Diola, D.; Dorin, G.; Ellens, K. W.; Fickes, S.; Galazzo, J.; Gaucher, S. P.; Geistlinger, T.; Henry, R.; Hepp, M.; Horning, T.; Iqbal, T.; Jiang, H.; Kizer, L.; Lieu, B.; Melis, D.; Moss, N.; Regentin, R.; Secrest, S.; Tsuruta, H.; Vazquez, R.; Westblade, L. F.; Xu, L.; Yu, M.; Zhang, Y.; ZHao, L.; Lievense, J.; Covello, P. S.; Keasling, J. D.; Reiling, K. K.; Renninger, N. S.; Newman, J.D. High-Level Semi-Synthetic Production of the Potent Antimalarial Artemisinin. *Nature* **2013**, *496* (7446), 528–532.

(46) Mori, T. Enzymatic Studies on Aromatic Prenyltransferases. *J. Nat. Med.* **2020**, *74* (3), 501–512.

(47) Ito, Y.; Terai, G.; Ishigami, M.; Hashiba, N.; Nakamura, Y.; Bamba, T.; Kumokita, R.; Hasunuma, T.; Asai, K.; Ishii, J.; Kondo, A. Exchange of Endogenous and Heterogeneous Yeast Terminators in *Pichia pastoris* to Tune mRNA Stability and Gene Expression. *Nucleic acids Res.* **2020**, *48* (22), 13000–13012.

(48) Kobayashi, Y.; Inokuma, K.; Matsuda, M.; Kondo, A.; Hasunuma, T. Resveratrol Production from Several Types of Saccharide Sources by a Recombinant *Scheffersomyces stipitis* Strain. *Metab. Eng. Commun.* **2021**, *13*, e00188.

For Table of Contents Use Only

Title:

***De novo* production of the bioactive phenylpropanoid artepillin C using membrane-bound prenyltransferase in *Komagataella phaffii*.**

Authors:

Takahiro Bamba[1,†], Ryosuke Munakata[2,†], Yuya Ushiro[3], Ryota Kumokita[3], Sayaka Tanaka[3], Yoshimi Hori[1], Akihiko Kondo[1,3,4], Kazufumi Yazakai[2,*], Tomohisa Hasunuma[1,3,4,*]

Table of contents (TOC) graphic

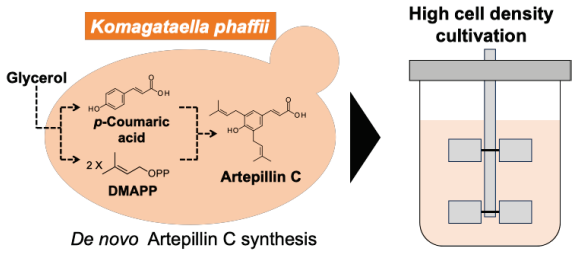

Fig. 1

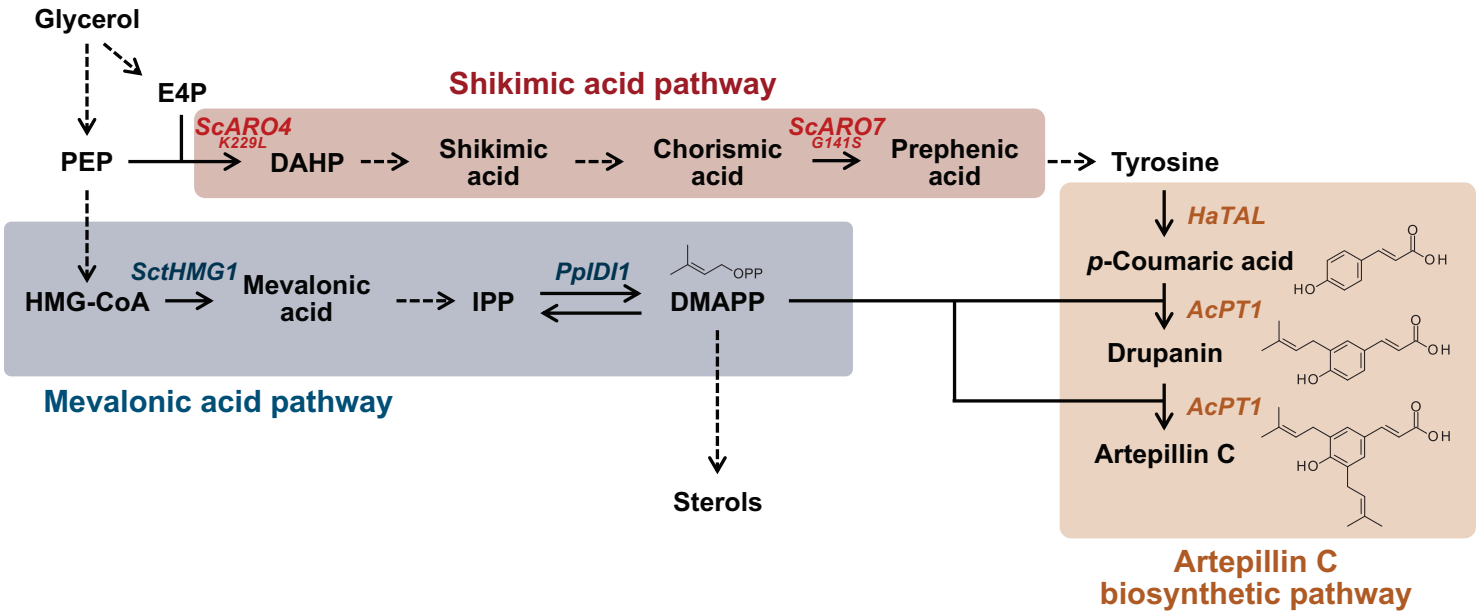

Figure 1. The biosynthetic pathway of artepillin C in *P. pastoris*.
Solid arrows indicate single reaction steps and the dashed arrows indicate multiple enzymatic steps. Abbreviations for metabolites and enzymes: PEP, phosphoenolpyruvate; E4P, erythrose 4-phosphate; DAHP, 3-deoxy-D-arabinoheptulosonate 7-phosphate; HMG-CoA, 3-hydroxy-3-methylglutaryl coenzyme A; IPP, isopentenyl pyrophosphate; DMAPP, dimethylallyl pyrophosphate; $ARO4^{K299L}$, a DAHP synthase mutant (K229L) from *S. cerevisiae*; $ARO7^{G141S}$, a chorismate mutase mutant (G141S) from *S. cerevisiae*; TAL, a tyrosine ammonia-lyase from *Herpetosiphon aurantiacus*; AcPT1, *Artemisia capillaris* prenyltransferase 1; tHMG1, an N-terminal truncated hydroxy-3-methylglutaryl coenzyme A reductase from *S. cerevisiae*; IDI1, an isopentenyl diphosphate delta isomerase from *P. pastoris*.

Fig. 2

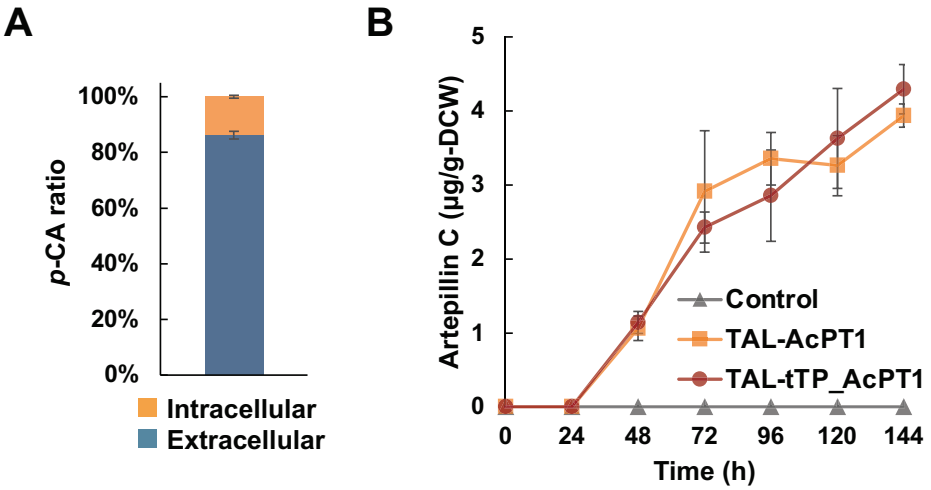

Figure 2. Engineering of *P. pastoris* expressing *TAL*.

(A) Ratio of intracellular and extracellular *p*-CA levels after 96 h of cultivation of *P. pastoris* strains overexpressing *TAL* in YPG medium. (B) Time course of intracellular artepillin C levels in YPG medium of engineered strains (TAL-AcPT1 and TAL-tTP_AcPT1) and a control strain (CBS7435*Δdnl4Δhis4*). All results are expressed as mean ± standard deviation of three biologically independent experiments.

Fig. 3

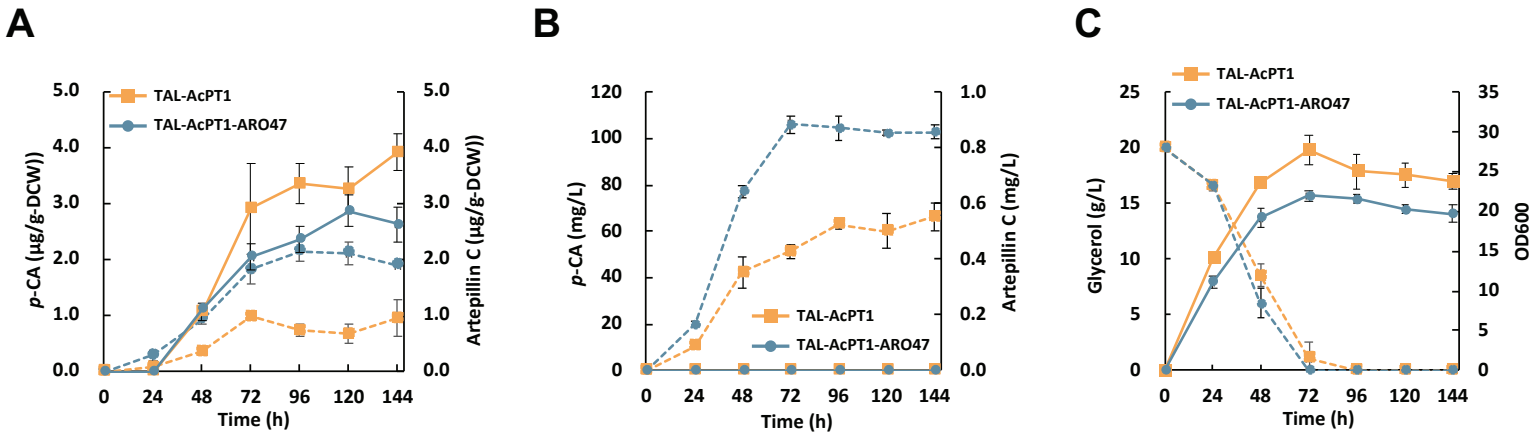

Figure 3. Artepillin C production by a *P. pastoris* strain overexpressing *ARO4*^{K299L} and *ARO7*^{G141S} (TAL-AcPT1-ARO47).

Time course of artepillin C (solid lines) and *p*-CA (dashed lines) production levels in the cell fraction (A) and the medium fraction (B). Cell growth (solid lines) and glycerol consumption (dashed lines) are shown in (C). Results are presented as mean ± standard deviation of three biologically independent experiments.

Fig. 4

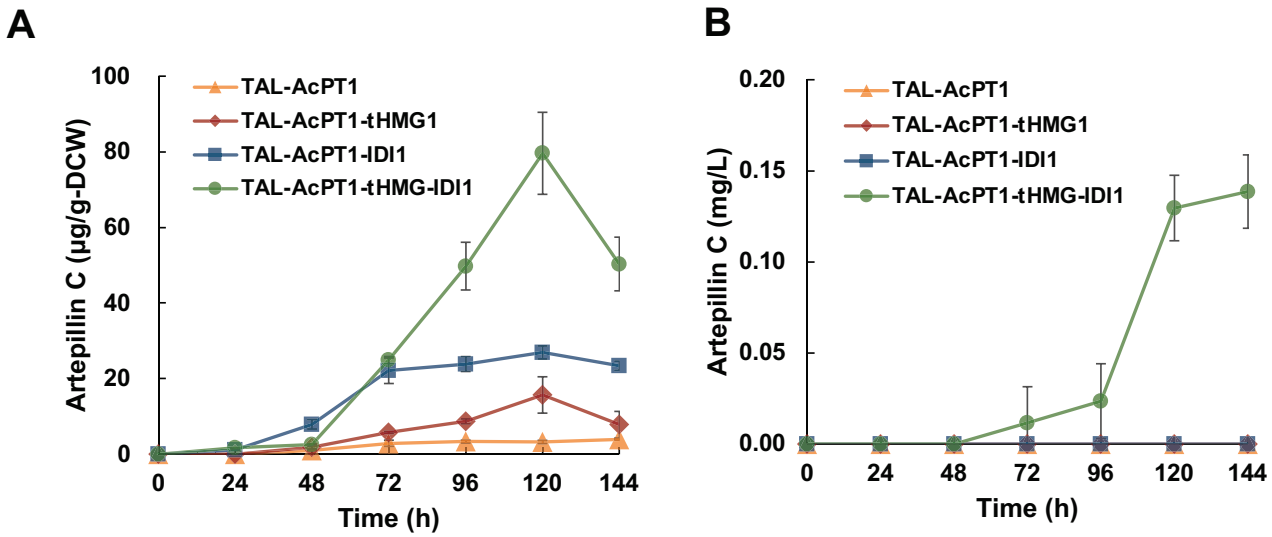

Figure 4. Artepillin C production by *P. pastoris* strains with enhanced DMAPP supply.

TAL-AcPT1-tHMG1, TAL-AcPT1-IDI1, and TAL-AcPT1-tHMG1-IDI1 were overexpressed in *P. pastoris*. Time courses of artepillin C production in the cell fraction (A) and that in the medium fraction (B). Results are presented as mean ± standard deviation of three biologically independent experiments.

Fig. 5

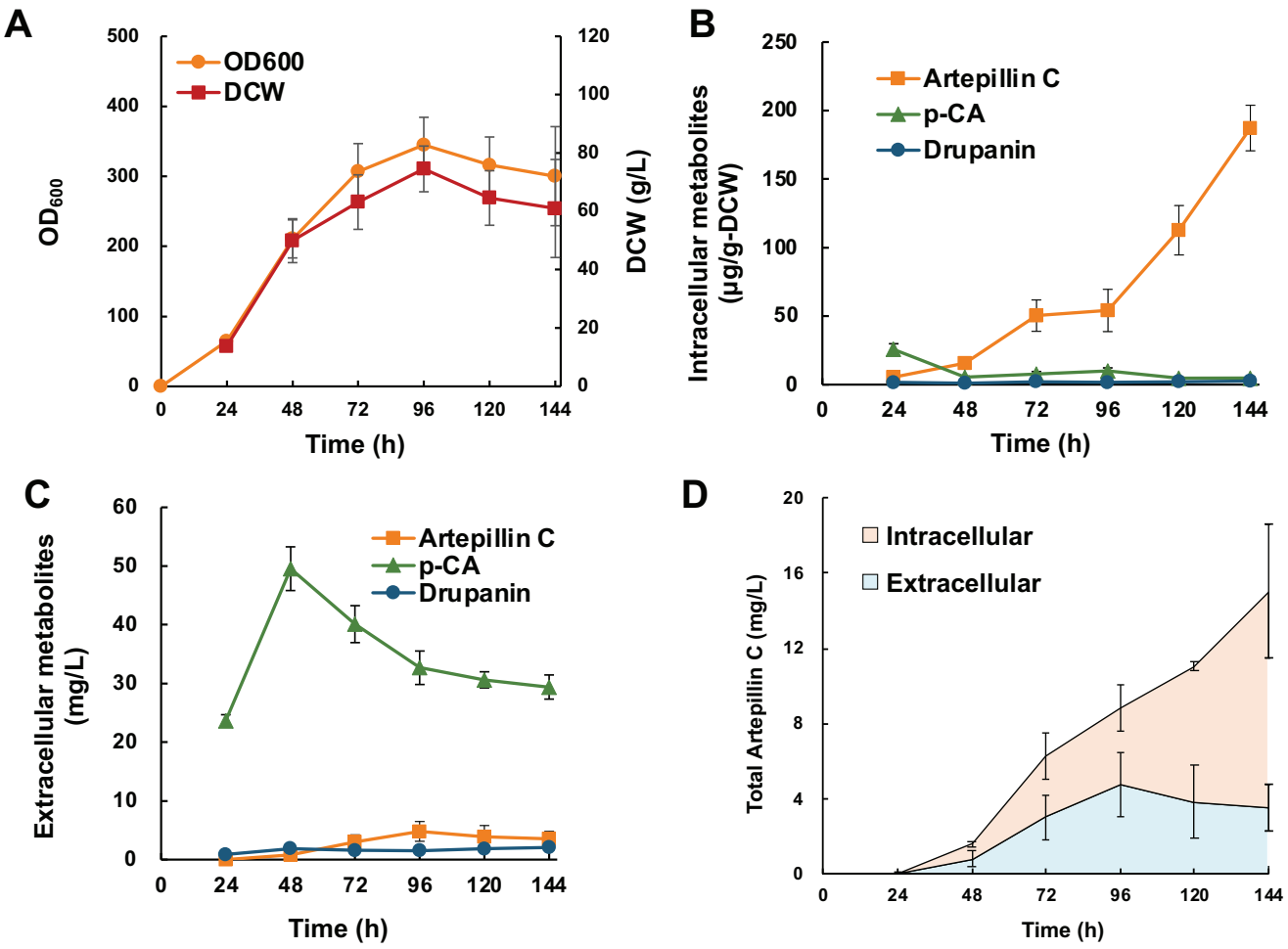

Figure 5. Fed-batch cultivation of the W-TAL-AcPT1-tHMG1-IDI1 strain with glycerol.

Time course monitoring of (A) OD_{600} and dry cell weight (DCW), (B) intracellular metabolites, (C) extracellular metabolites, and (D) the total artepillin C level. Results are presented as mean ± standard deviation of three biologically independent experiments.

Fig. 6

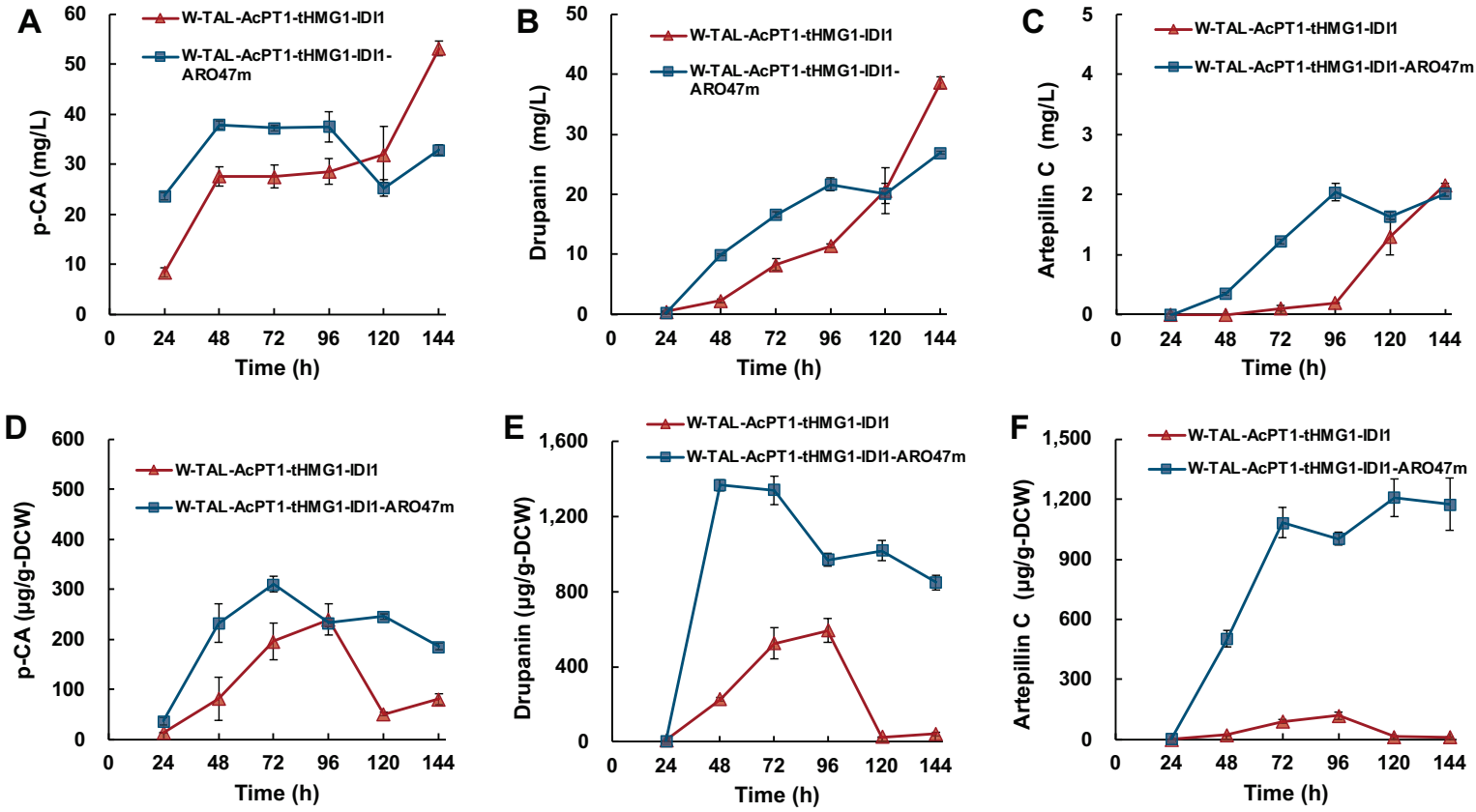

Figure 6. Artepillin C production by *K. phaffii* strains with enhanced DMAPP and *p*-CA *in vivo* supply.

Time course of intracellular amounts of (A) *p*-CA, (B) drupanin, and (C) artepillin C, and extracellular amounts of (D) *p*-CA, (E) drupanin, and (F) artepillin C. Results are presented as mean ± standard deviation of three biologically independent experiments.